Synthesis of superheavy nuclei: Nucleon collectivization as a mechanism for compound nucleus formation

V. I. Zagrebaev

Flerov Laboratory of Nuclear Reaction, JINR, Dubna, Moscow Region, Russia

A consistent systematic analysis of the synthesis of very heavy nuclei is performed within a "standard" theoretical approach without any adjustable parameters and additional simplification. Good agreement with experimental data was obtained in all the cases up to synthesis of the 102 element. It was confirmed that a process of the compound nucleus formation, starting from the instant when two heavy nuclei touch and proceeding in strong competition with the fission and quasifission processes, plays an important role in the asymmetric synthesis of superheavy elements with $Z_{CN} \geqslant 104$ as well as in the symmetric fusion at $Z_{CN} \geqslant 90$. A new mechanism of the fusion-fission process for a heavy nuclear system is proposed, which takes place in the (A_1, A_2) space, where A_1 and A_2 are two nuclei, surrounded by a certain number of common nucleons ΔA. These nuclei gradually lose (or acquire) their individualities with increasing (or decreasing) the number of collectivized nucleons ΔA. The driving potential in the (A_1, A_2) space is derived, which allows the calculation of both the probability of the compound nucleus formation and the mass distribution of fission fragments in heavy ion fusion reactions.

I. INTRODUCTION

The interest in the problem of the synthesis of superheavy atomic nuclei quickened significantly within the past two years. First of all, it is connected with successful Dubna experiments on the synthesis of the 114 element isotopes with $A = 288,289$ [1] and $A = 287$ [2]. The decay chains of these isotopes demonstrate that we have really approached the so-called "island of stability." Shortly after these experiments, the detection of nuclei with $Z = 118$ was announced at Berkeley in the ^{86}Kr$+^{208}$Pb fusion reaction with an unexpectedly large cross section [3]. As a result, two other laboratories (RIKEN and GANIL) joined the well-known centers in the synthesis of superheavy elements (Berkeley, Darmstadt, and Dubna). Detailed information on the synthesis of superheavy elements (SHEs) including the latest discoveries and the current status of the problem can be found in [4]. Today at all the above mentioned laboratories either experiments or intensive preparatory work are in progress. Theoretical support of these very expensive experiments is vital in the choice of fusing nuclei and their collision energy, and for the estimation of the cross sections and identification of evaporation residues. In this connection, one should recognize the fact that we are still far from final understanding of the heavy ion fusion process, which is of independent scientific interest from the point of view of the study of properties and behavior of nucleon and collective degrees of freedom in low excited nuclear systems.

The fusion dynamics undergoes significant changes with increasing masses of compound nuclei, and the formation cross sections decrease very fast with increasing their atomic numbers. The main reason for that is the growing role of the fission channels determining not only the survival probability of a compound nucleus in the process of its cooling (emission of nucleons and γ rays), but also the dynamics of its formation in competition with the so-called quasifission process. The physics nature of the whole process of the interac-

tion of two heavy nuclei leading to formation of a heavy evaporation residue or two fission fragments is very complicated even at low near-barrier energies. As a result, not very numerous theoretical approaches to the description of the synthesis of SHEs differ from each other not only quantitatively (several orders of magnitude in the estimation of the cross sections of the same processes) but, sometimes, qualitatively, namely, when contradictory physics models are used.

The formation cross section of a cold residual nucleus B, which is the product of light particle evaporation and γ emission from an excited compound nucleus C, formed in the fusion process of two heavy nuclei $A_1 + A_2 \rightarrow C \rightarrow B + n, p, \alpha, \gamma$ at center-of-mass energy close to the Coulomb barrier in the entrance channel, can be decomposed over partial waves and written in the following form:

$$\sigma_{ER}^{A_1+A_2 \rightarrow B}(E) \approx \frac{\pi \hbar^2}{2\mu E} \sum_{l=0}^{\infty} (2l+1) T(E,l) P_{CN}$$
$$\times (A_1+A_2 \rightarrow C; E,l) P_{ER}(C \rightarrow B; E^*, l). \quad (1)$$

Here $T(E,l)$ is the probability for colliding nuclei to overcome the potential barrier in the entrance channel and reach the point of contact $R_{cont} = R_1 + R_2$, which is, as a rule, less than the radius of the Coulomb barrier R_C^B by 2 or 3 fm, R_1 and R_2 are the radii of the nuclei. P_{CN} is the probability that the nuclear system will evolve from a configuration of two touching nuclei into a spherical or nearly spherical form of the compound mononucleus. In the course of this evolution the heavy system may, in principle, fall again into two fragments without forming the compound nucleus (quasifission) and, thus, $P_{CN} \leqslant 1$. The last term in Eq. (1), $P_{ER}(C \rightarrow B)$, defines the probability of producing the cold evaporation residue B in the process of the compound nucleus C decay. It has the initial excitation energy $E^* = E - Q_{gg}^{fus}$, where E is the beam energy in the center-of-mass system, Q_{gg}^{fus}

$= M(C)c^2 - M(A_1)c^2 - M(A_2)c^2$, and $M(C)$, $M(A_1)$, $M(A_2)$ are the nuclear masses. In order to avoid hereinafter a confusion in terminology, we define also the "capture cross section" and the "fusion cross section" as follows:

$$\sigma_{capt}(E) = (\pi\hbar^2/2\mu E)\sum_{l=0}^{\infty}(2l+1)T(E,l),$$

$$\sigma_{fus}(E) = (\pi\hbar^2/2\mu E)\sum_{l=0}^{\infty}(2l+1)T(E,l)P_{CN}(E,l).$$

Approximate equality in Eq. (1) reflects the fact that the whole process of the compound nucleus formation and decay is divided here into three individual reaction stages even if connected with each other but treated and calculated separately: (1) approaching the point of contact $R_1 + R_2 \leqslant r < \infty$, (2) formation of the compound mononucleus $A_1 + A_2 \rightarrow C$, (3) decay ("cooling") of the compound nucleus C. Note that different theoretical approaches are used for analyzing all the three reaction stages. However, the dynamics of the intermediate stage of the compound nucleus formation is the most vague. It is due to the fact that in a well studied case of near-barrier fusion of light and medium nuclei, when a fissility of a compound nucleus is not so high, the fusing nuclei overcoming the potential barrier form a compound nucleus with a probability close to unity, i.e., $P_{CN} = 1$, $\sigma_{fus} = \sigma_{capt}$, and, thus, this reaction stage does not influence the yield of the evaporation residues at all. In the fusion of heavy nuclei, the system may evolve with a high probability directly into the exit fission channel without the compound nucleus formation, which means that the so-called process of "fast fission" or quasifission takes place [5]. Dynamics of the whole process is rather complicated, and that is why very much different models, sometimes opposite in their physical meaning, are used for its description.

In this connection, one may single out two mutually exclusive approaches to the description of the evolution of the nuclear system starting from the moment at which two colliding nuclei touch each other and up to the moment of formation of a spherical compound nucleus or the moment of decay into two more or less equal heavy fragments (quasifission process). In the first approach [6–8] it is assumed that two touching nuclei instantly and completely lose their individualities and can be treated as one strongly deformed mononucleus that evaluates in the multidimensional space of deformations into a spherical compound nucleus or goes into fission channels. In practice one has to use a few collective degrees of freedom defining the shape of the nuclear system and completely neglect the shell structure of the nuclei, i.e., their individuality, playing an important role at low excitation energies. Similar models were also used in [9,10] for the description of the intermediate reaction stage of the compound nucleus formation in specific calculations of the cross sections of SHE production.

An opposite approach has been proposed and used in [11–13]. Here, two nuclei having passed the Coulomb barrier reach the point of contact and, after that, remain in this position keeping entirely their individualities and shapes. Only

nucleon transfer causes subsequent evolution of the "dinuclear system." Compound nucleus formation means complete transfer of all the nucleons from the light nucleus to the heavier one. This process competes with the nucleon transfer from the heavy nucleus to the lighter one, resulting in a subsequent separation of two nuclei (quasifission process).

The truth seems to be somewhere in the middle. It is improbable that during the whole evolution of the system starting from the touching of two nuclei and up to the formation of the almost spherical compound nucleus, all the nucleons were strictly divided into two groups, namely, the nucleons belonging only to one nucleus and moving only in the volume of that nucleus, and those belonging to another nucleus and also remaining within its volume. The process of instantaneous nucleon collectivization and formation of one very strongly deformed mononucleus at the moment of contact of two colliding nuclei also looks unlikely to take place. In this paper a new mechanism of compound nucleus formation is proposed. It is assumed that a certain number of common nucleons appear when two nuclei get in contact. These nucleons move within the whole volume occupied by the nuclear system and belong to both nuclei. Henceforth the number of such collectivized nucleons increases whereas the number of nucleons belonging to each particular nucleus decreases. The compound nucleus is formed at the instant when all the nucleons find room in the volume of that nucleus. The inverse process of nucleon decollectivization brings the system to the fission channels.

A mechanism of compound nucleus formation is discussed in detail in Secs. V and VI, whereas Secs. II–IV are devoted to the resources and applicability of the "standard approach" to the description of the SHE synthesis. Here the stage of compound nucleus formation is neglected, i.e., $P_{CN} = 1$ and the main attention is focused on the interaction of two heavy nuclei, on overcoming the multidimensional potential barrier, and on the cooling process of a low excited fissile compound nucleus.

II. THE STAGE OF APPROACHING AND THE CAPTURE CROSS SECTION

In fact many difficulties arise both in the calculation of P_{CN} in Eq. (1) and in the calculation of other factors. Now it is well established that in the fusion of heavy ions the barrier penetrability $T(E,l)$ is defined not only by the height and width of the Coulomb barrier but also by the strong channel coupling of relative motion with internal degrees of freedom, which enhances significantly (by several orders of magnitude) the fusion cross section at sub-barrier energies (see, e.g., [14]). In the case when the capture cross section is measured experimentally within a not-so-narrow near-barrier energy region, the height of the potential barrier and the so-called "barrier distribution function" can be obtained from experimental data, and the transmission coefficients $T(E,l)$ can be easily calculated or approximated. In the synthesis of SHEs it is difficult to measure the capture cross section $\sigma_{capt}(E)$ (it can be done by detecting the yield of fission fragments) and the barrier penetrability $T(E,l)$ has to be

estimated within some theoretical model describing the initial stage of the reaction.

The Bass approximation of potential energy of the interaction between two heavy spherical nuclei [15] is widely used and reproduces rather well the height of the potential barrier. Coupling with the surface vibrations and nucleon transfer channels is the second main factor that determines the capture cross section at near-barrier energies [14]. In the case of rather ''soft'' nuclei (low energy values of the vibrational excitations) a realistic nucleus-nucleus interaction leads to very large deformations and, thus, to a necessity of taking into account a large number of coupled channels [16], which significantly complicates the microscopic calculation of $T(E,l)$ and makes it unreliable.

In order to take into account explicitly the main effect of a decrease in the height of the potential barrier and, therefore, an increase in the penetration probability at sub-barrier energies due to dynamic deformation of nuclear surfaces, we use here the following nucleus-nucleus potential energy for nuclei with quadrupole deformations in a nose-to-nose geometry

$$V_{1,2}(r,\beta_1,\beta_2) = V_C(r,\beta_1,\beta_2) + V_{prox}(r,\beta_1,\beta_2)$$
$$+ \tfrac{1}{2}C_1(\beta_1-\beta_1^0)^2 + \tfrac{1}{2}C_2(\beta_2-\beta_2^0)^2. \quad (2)$$

Here numbers 1 and 2 denote the projectile and the target, $\beta_{1,2}$ are the parameters of the dynamic quadrupole deformation, $\beta_{1,2}^0$ are the parameters of static deformation, and $C_{1,2}$ are the stiffness parameters, which were calculated within the liquid drop model. The diffuseness parameter b of the proximity potential [17] was taken as equal to 1 fm for all nuclei except for light projectiles such as ^{12}C and ^{16}O, for which it was chosen as 1.1 fm. Calculating the proximity forces we also take into account a change in the surface curvature of deformed nuclei. Nuclear radii were calculated with $r_0=1.16$ fm. In the case of the zero deformation $\beta=0$ this potential yields the Coulomb barriers that are slightly higher than the Bass barriers, whereas the saddle points locate, as a rule, much lower than the Bass barriers: $B_S \equiv V_{12}(r=r_{sd},\beta=\beta_{sd}) < B_{Bass}$. To reduce the number of variables we assume that the deformation energies of two nuclei are proportional to their masses, i.e., $C_1\beta_1^2/C_2\beta_2^2 = A_1/A_2$, and we may use only one deformation parameter $\beta=\beta_1+\beta_2$.

A characteristic topographical landscape of the total (Coulomb, nuclear, and deformational) potential energy of the nucleus-nucleus interaction in the (r,β) space is shown in Fig. 1(a). The interaction potential of spherical nuclei ($\beta=0$) and potential energy along the ridge of the multidimensional barrier [dotted line in Fig. 1(a)] are shown in Figs. 1(b) and 1(c), respectively. The big gray-shaded arrow sche-

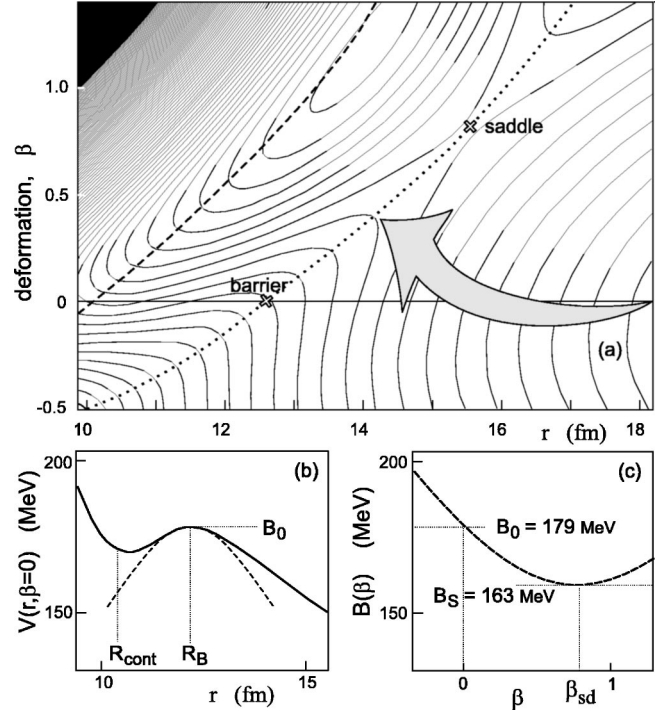FIG. 1. Potential energy of $^{48}Ca + ^{208}Pb$. Proximity potential is used for the nuclear interaction ($r_0=1.15$ fm, $b=1.0$ fm), and the standard stiffness parameter is used for the deformation energy. (a) Landscape of potential surface. The saddle point and the potential barrier of spherical nuclei ($\beta=0$) are shown by the crosses. The ridge of the barrier is shown by the dotted line, whereas the dashed line corresponds to the contact distance of two nuclei. The incoming flux is shown schematically by the gray-shaded arrow. (b) Interaction potential of spherical nuclei and its parabolic approximation (dashed line) in the vicinity of the barrier. (c) Potential energy at the ridge of the two-dimensional barrier, i.e., along the dotted line passing through the saddle point [see (a)].

matically shows the incoming flux, which overcomes the barrier at different values of dynamic deformation. A quantum and classical analysis of this process performed for a model system can be found in [16]. In order to determine the quantum penetrability of such barrier one needs to solve a multidimensional Schrödinger equation. However, approximating the radial dependence of the barrier by a parabola [see Fig. 1(b)], one can use the usual Hill-Wheeler formula [18] with the barrier height modified to include a centrifugal term for the estimation of the quantum penetration probability of a one-dimensional potential barrier. Taking into account now a multidimensional character of the realistic barrier, we may introduce the ''barrier distribution function'' [19] $f(B)$ in order to determine its total penetrability

$$T(E,l) = \int f(B) \frac{1}{1+\exp\left(\dfrac{2\pi}{\hbar\omega_B(l)}\left[B+\dfrac{\hbar^2}{2\mu R_B^2(l)}l(l+1)-E\right]\right)} dB. \quad (3)$$

Here $\hbar\omega_B$ is defined by the width of the parabolic barrier, R_B defines a position of the barrier, and the barrier distribution function satisfies the normalization condition $\int f(B)dB = 1$. At an accurate measurement of the capture cross section $\sigma_{capt}(E)$ this function can be determined experimentally [14]. In other cases we rely only on available experimental experience and theoretical analysis of model systems. Here the asymmetric Gaussian approximation of this function was used

$$f(B) = N \times \begin{cases} \exp\left[-\left(\dfrac{B-B_m}{\Delta_1}\right)^2\right], & B < B_m \\ \exp\left[-\left(\dfrac{B-B_m}{\Delta_2}\right)^2\right], & B > B_m, \end{cases} \quad (4)$$

where $B_m = (B_0 + B_S)/2$, B_0 is the height of the barrier at zero deformation, B_S is the height of the saddle point (see Fig. 1), $N(\Delta_1,\Delta_2)$ is the normalization coefficient, and $\Delta_2 = (B_0 - B_S)/2$. Experiments (see, e.g., [14]) and theoretical analysis show that the value of Δ_1 is, as a rule, less than the value of Δ_2 and in all the cases considered below it was taken as equal to 2 MeV.

III. STATISTICAL DECAY OF LOW EXCITED HEAVY NUCLEI

The survival probability of the excited compound nucleus $C(E^*,J)$ in the process of its cooling by means of neutron evaporation and γ emission in the competition with fission and emission of light charged particles can be calculated within a statistical model of atomic nuclei [20]. The standard expressions were used for the partial decay widths of the compound nucleus $\Gamma_{C\to B+a}(E^*,J)$, $\Gamma_\gamma^L(E^*,J)$, and $\Gamma_{fis}(E^*,J)$ [15,20,21] with the level density, which includes the collective enhancement factor proposed in [22]. The fission barrier was calculated as $B_{fis}(E^*) = B_{LD} - \delta W e^{-\gamma_D E^*}$, where B_{LD} is the LDM fission barrier, δW is the shell correction energy calculated for the nucleus in its ground state (we ignore here the shell effects at the saddle point), and γ_D is the damping parameter describing a decrease in the shell effects in an energy level density with increasing the excitation energy of the nucleus. The value of this parameter is especially important in the case of superheavy nuclei, the fission barriers of which are determined mainly just by the shell corrections to their ground states. In literature one can find close but slightly different values of the damping parameter. Here the value $\gamma = 0.061$ MeV^{-1} is used taken from [23] where it was derived from a systematic description of the energy level density over a wide range of nuclei.

Subsequent estimation of the total probability for the formation of the cold residual nucleus after the emission of x neutrons—$C \to B + xn + N\gamma$—is usually performed within numerical calculations based on the analysis of the multistep decay cascade [24–26]. In this paper an explicit analytic expression is used for such probability, which takes into account directly the Maxwell-Boltzmann energy distribution of evaporated neutrons

$$P_{ER}(C \to B + xn)$$

$$= \int_0^{E_0^* - E_n^{sep}(1)} \frac{\Gamma_n}{\Gamma_{tot}}(E_0^*,J_0)P_n(E_0^*,e_1)de_1$$

$$\times \int_0^{E_1^* - E_n^{sep}(2)} \frac{\Gamma_n}{\Gamma_{tot}}(E_1^*,J_1)P_n(E_1^*,e_2)de_2\cdots$$

$$\times \int_0^{E_{x-1}^* - E_n^{sep}(x)} \frac{\Gamma_n}{\Gamma_{tot}}(E_{x-1}^*,J_{x-1})P_n(E_{x-1}^*,e_x)$$

$$\times G_{N\gamma}(E_x^*,J_x \to \text{g.s.})de_x. \quad (5)$$

Here $E_n^{sep}(k)$ and e_k are the binding and kinetic energies of the kth evaporated neutron, $E_k^* = E_0^* - \Sigma_{i=1}^k [E_n^{sep}(i) + e_i]$ is the excitation energy of the residual nucleus after the emission of k neutrons, $P_n(E^*,e) = C\sqrt{e}\exp[-e/T(E^*)]$ is the probability for the evaporated neutron to have energy e, and the normalizing coefficient C is found from the condition $\int_0^{E^* - E_n^{sep}} P_n(E^*,e)de = 1$. The quantity $G_{N\gamma}$ defines the probability for the remaining excitation energy and angular momentum to be taken away by γ emission after evaporation of x neutrons. It can be approximated by the expression

$$G_{N\gamma}(E^*,J \to \text{g.s.}) = \prod_{i=1}^N \frac{\Gamma_\gamma(E_i^*,J_i)}{\Gamma_{tot}(E_i^*,J_i)}, \quad (6)$$

where $E_i^* = E^* - (i-1)\langle e_\gamma \rangle$, $J_i = J - (i-1)$, $\langle e_\gamma \rangle$ is the average energy of a dipole γ quantum, and the number of γ quanta N is determined from the condition $E_N^* < B_{fis}$, assuming that at energies lower than the fission barrier the fission probability is very small as compared with γ emission, and $\Gamma_\gamma/\Gamma_{tot} \approx 1$. Numerical calculations show that a choice of the average energy of the emitted γ quanta $\langle e_\gamma \rangle$ in the range 0.1–2.0 MeV weakly influences the final results in all the cases except for the $0n$ fusion channel, the cross section of which is negligibly small in the reactions considered here.

IV. "STANDARD APPROACH"—THE BORDERLINES OF APPLICABILITY

As mentioned above, at low energies in comparatively light systems the formation of a compound nucleus occurs with a probability close to unity straight after overcoming the Coulomb barrier. Let us call this approach "standard," when in the calculation of the cross section of the evaporation residue formation (1) the value of $P_{CN} = 1$ is used. In this section the standard approach is applied to the analysis of available experimental data on the synthesis of very heavy fissile nuclei in order to find the borderlines of applicability of this approach, i.e., to find the cases in which the intermediate reaction stage, i.e., the competition between compound nucleus formation and quasifission after two colliding nuclei touch, plays an important role and significantly decreases the yield of the superheavy nuclei.

To avoid adjustment of the calculated and experimental data by playing with parameters, the same scheme of the calculation of $T(E,l)$ and $P_{ER}(C \to B + xn)$ described above

was used in all the cases. Besides the neutron evaporation, γ emission and fission, the evaporation of protons and α particles was also taken into account in the calculation of the total decay width Γ_{tot} used in the neutron cascade. Experimental nuclear masses [27] were used to determine the separation energies of all the light particles. The fission barriers of formed nuclei $B_{fis}(A;E^*,J)$ are the most important and most uncertain parameters of the calculation. Theoretical estimations of the fission barriers for the region of superheavy nuclei are not very reliable yet and significantly differ from each other (e.g., compare the results given in [29,30] and in [31]). To make the analysis consistent, the liquid drop fission barriers [28] and shell corrections [29,30] obtained within similar approaches were used in all the cases considered here.

Satisfactory agreement of the standard approach with experimental data was obtained for many asymmetrical fusion reactions leading to formation of heavy fissile nuclei with $90 \leqslant Z_{CN} \leqslant 102$, which allows one to conclude about applicability of the used approach to description of such reactions. Analysis of the ^{48}Ca+^{208}Pb fusion reaction is a nice test of correct choice of all the parameters. The decay properties of nobelium isotopes produced in this reactions are already very close to the properties of superheavy nuclei. The liquid drop part of the fission barrier is, here, about 1.2 MeV, and B_{fis} is determined mainly by the shell effects. Thus, the role of the shell correction and its damping with increasing the excitation energy can be studied here quite accurately. In the calculations of the fission barriers of nobelium isotopes we used the shell corrections to their ground states proposed in [30] and found that those barriers along with experimental values of neutron separation energies reproduce sufficiently well the corresponding survival probabilities [33] (Fig. 2).

However, already for the elements with $Z_{CN}=104$, synthesized in the reaction ^{50}Ti+^{208}Pb$\rightarrow$^{258}Rf, the standard approach overestimates the cross section for the yield of evaporation residues (ER) if one uses the fission barriers calculated on the basis of shell corrections taken from [29,30], see Fig. 3. The discrepancy between calculated and experimental ER cross sections is much more for the reaction ^{58}Fe+^{208}Pb $\rightarrow$^{266}Hs (Fig. 4) [35].

There are two possible reasons for such overestimation.

(i) Neglecting an intermediate reaction stage of the compound nucleus formation in competition with quasifission, i.e., a necessity of calculating and taking into account the factor $P_{CN}<1$ in the total cross section (1).

(ii) Overestimation of the fission barriers of superheavy nuclei in the calculation of the survival probability $P_{ER}(C \rightarrow B+xn)$. Starting from $Z_{CN}=106$ the shell corrections given in [29,30] begin to increase due to the approaching magic shell in the region of $Z=114$ and $N=184$, whereas the neutron separation energies do not decrease at least in the fusion reactions induced by stable projectiles and targets. If the static fission barriers are defined directly by the ground state shell correction energies, as made here and in many other papers, then the survival probabilities, as calculations show, stop decreasing with increasing Z_{CN} at $Z_{CN}>106$, while the experiments demonstrate a systematic decrease in the yield of the superheavy evaporation residues with in-
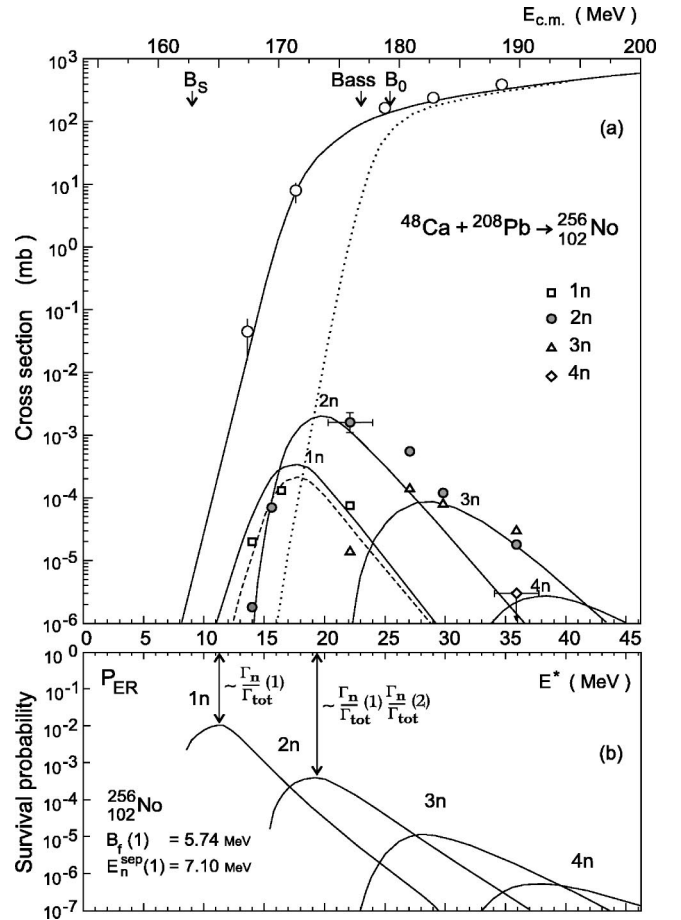

FIG. 2. (a) The capture cross section and formation cross sections for evaporation residues in the ^{48}Ca+^{208}Pb reaction. The dotted curve shows the capture cross section calculated without dynamic deformation of nuclei. By the arrows are shown the positions of the Coulomb barrier at zero deformation, the Bass barrier, and the saddle point. Experimental data are from [32] (capture cross sections) and from [33] (cross sections of the xn channels). For the yields of evaporation residues the error bars are shown only for two energies to avoid overloading the picture. The dashed curve corresponds to the calculation with $P_{CN}<1$ (see Fig. 11 and the text). (b) Survival probabilities of the compound nucleus ^{256}No after the evaporation of 1,2,3, and 4 neutrons at the initial angular momentum $J=0$.

creasing Z_{CN} [4]. Both the high probability for the system to go into the quasifission channels and decreasing the height of the real fission barriers, in spite of the large values of the shell correction energies near the magic shells, could be the reasons for that.

To make, finally, sure that the stage of the compound nucleus formation and the quasifission process should be considered much more carefully in the synthesis of superheavy nuclei, the symmetric fusion reactions leading to the heavy fissile compound nuclei, fission barriers of which are known much better, have been also analyzed within the standard approach. Comparison of the calculated and experimental cross sections for the yield of evaporation residues in such reactions as ^{100}Mo+^{110}Pd$\rightarrow$^{210}Ra, ^{86}Kr+^{136}Xe$\rightarrow$^{222}Th, and ^{96}Zr+^{124}Sn$\rightarrow$^{220}Th shows that the calculated cross sections
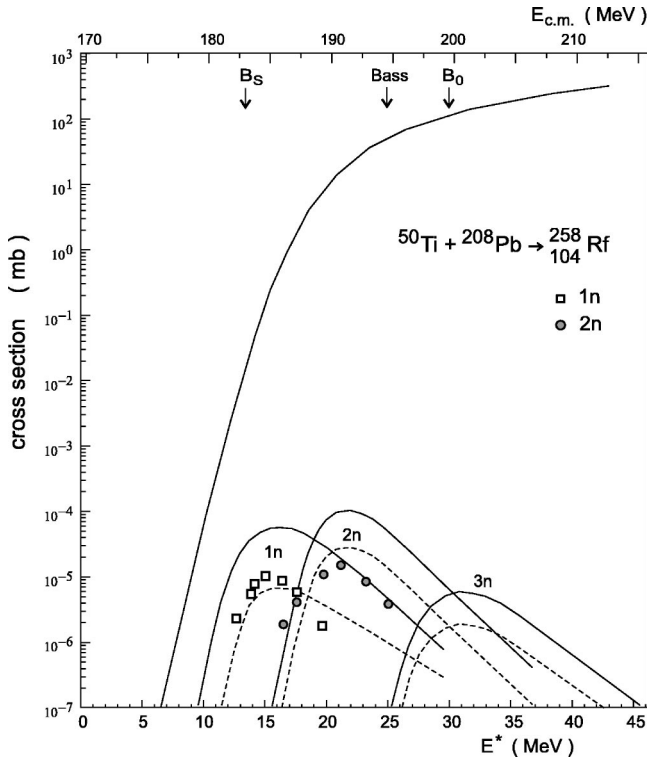
FIG. 3. The capture cross section and formation cross sections for evaporation residues in the ^{50}Ti$+^{208}$Pb fusion reaction. Experimental cross sections for the $1n$ and $2n$ channels are from [34]. Notations are the same as in Fig. 2.

FIG. 4. The same as in Fig. 2 but for the ^{58}Fe$+^{208}$Pb reaction leading to formation of the element with $Z=108$. Experimental data are from [35] (the capture cross sections) and from [34] ($1n$ ER cross sections).

noticeably overestimate the experimental data at low near-barrier energies and rather well agree with experiments at higher energies, in the region of the $4n$ channel and higher. It means, that the survival probabilities are calculated quite accurately for these cases and an additional decrease in the experimental cross sections at low incident energies is most probably due to a reluctance of the two touching heavy nuclei close in masses to form a compound nucleus. They prefer to go into the initial channel or into some fission channels close to the entrance one, which means the well-known extra-push effect [36].

Thus, we may conclude with much certainty that in heavy ion fusion reactions the competition between the process of the compound nucleus formation and the process of quasifission, starting from the instant when two nuclei touch, plays an important role at $Z_{CN}\geq 104$ in collisions of asymmetric nuclei, and already at $Z_{CN}\geq 90$ in extremely symmetric combinations of colliding nuclei. For symmetric combinations this competition is especially noticeable at slow collisions, i.e., at near-barrier energies.

V. NUCLEON TRANSFER IN HEAVY ION FUSION REACTIONS

As mentioned above, there are two contradictory concepts of the compound nucleus formation. One of them assumes that all the nucleons are instantly collectivized straight after a touch of two nuclei forming one strongly deformed mononucleus, which gradually acquires a spherical shape in the
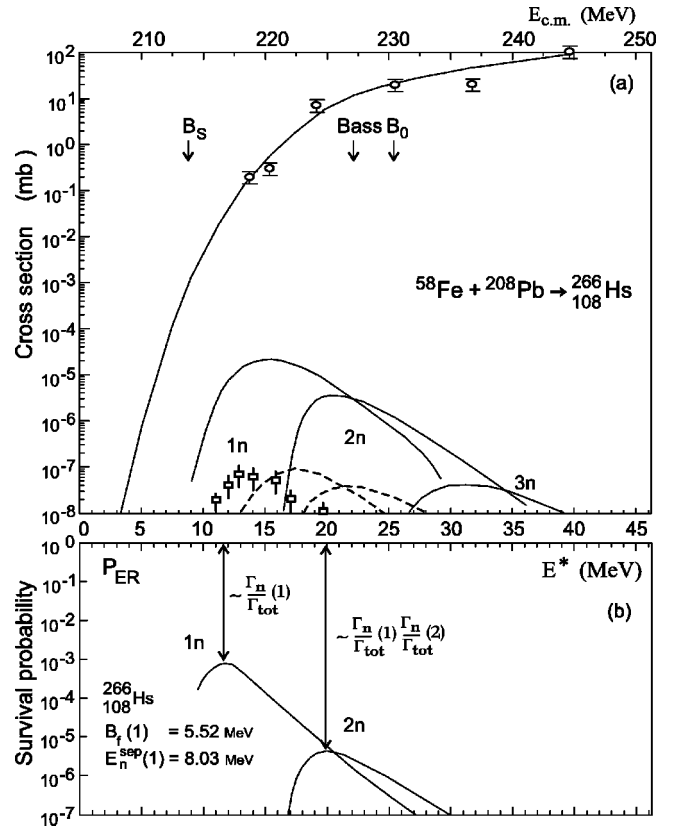
space of deformation parameters. The other assumes that two touching nuclei keep their individualities until the end, i.e., until one of them, the lightest, has transferred all its nucleons to another nucleus.

To understand clearly the mechanism of the nucleon transfer and collectivization in heavy ion collisions, a many-particle nonstationary Schrödinger equation should be solved using the realistic interaction potentials and realistic channel coupling. It is rather difficult to perform, if it is possible at all. Instead of that we tried to analyze the behavior of nucleons during the stage of approaching within a simplified four-body classical model consisting of two heavy nuclear cores and two valence nucleons, one inside each of the nuclei at the initial moment. Realistic Woods-Saxon potentials were used for the nucleon-nucleus interaction, and the proximity potential along with phenomenological dissipative forces were used for the nucleus-nucleus interaction. Here the time evolution of the system and the probability of nucleon collectivization at different collision stages were studied. This probability can be defined in the following way. Let N_{tot} be the number of all the events with randomly chosen initial configurations of colliding nuclei at fixed separation energies and angular moments of nucleons and at a given initial energy of relative motion. By the moment t in the case of the ΔN_1 events the nucleon has passed from the projectile into the target and is inside it, and in the case of the ΔN_2 events the nucleon has passed from the projectile into the target but
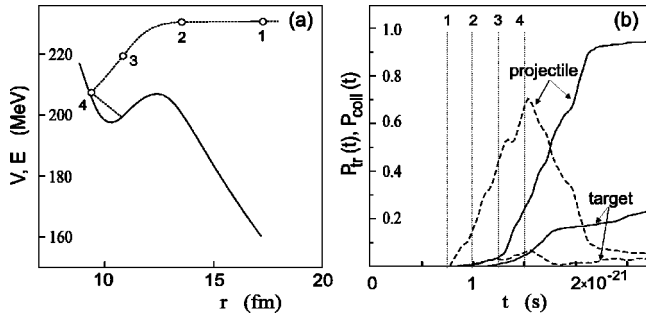
FIG. 5. (a) The interaction potential and relative motion trajectory for the collision of ^{48}Ca and ^{248}Cm at the energy $E_{cm} = 230$ MeV. (b) Probabilities of the valence neutron transfer (dashed lines) and neutron collectivization (solid lines). Dotted lines and numbers correspond to the moments shown on the left panel.

has returned, i.e., it has crossed at least twice the surface of the projectile. Then $P_{tr}(t) = \Delta N_1(t)/N_{tot}$ is the probability of the nucleon transfer, and $P_{coll}(t) = \Delta N_2(t)/N_{tot}$ is the probability of the nucleon collectivization. Similarly these probabilities are defined for the target nucleons.

As an example the fusion of ^{48}Ca with ^{248}Cm was studied at a near-barrier energy. One of the trajectories in the $(r, E_{c.m.})$ space and time evolution of the probabilities for transfer and collectivization of the projectile and target valence neutrons is shown in Fig. 5. In Fig. 6 typical trajectories of the neutrons are shown starting from the moment t_1 corresponding to position 1 in Fig. 5.

As the calculations show the probability of nucleon collectivization begins to increase immediately after overcoming the Coulomb barrier, and after the contact between the nuclear surfaces it rapidly reaches the value close to unity in the case of the nucleons of the light nucleus and a slightly less value in the case of the heavier partner nucleons. The last mentioned case is due to a smaller value of the ratio of the surface of the open window to the surface of the whole nucleus, inside which the transferred nucleon is initially situated. Later all the valence nucleons are moving in the volume of both nuclei (see Fig. 6), whereas the internal nucle-
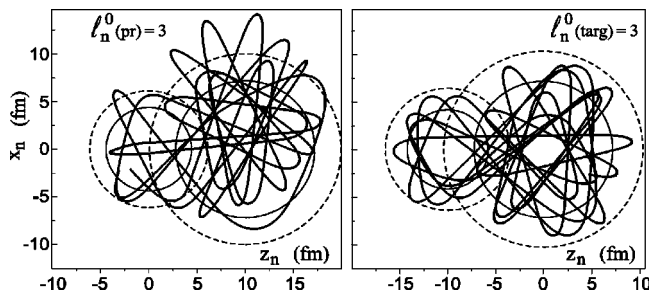

FIG. 6. Trajectories of valence neutrons of the projectile (left panel) and target (right panel) in the collision of ^{48}Ca with ^{248}Cm at $E_{c.m.} = 230$ MeV. Initial neutron angular moments are equal to $3\hbar$ for both nuclei, and initial neutron energies are taken in accordance with their experimental binding energies. The circles show the radii of the nuclei and the radii of valence neutron orbits. The trajectories are shown from the moment t_1, marked by number 1 in Fig. 5.
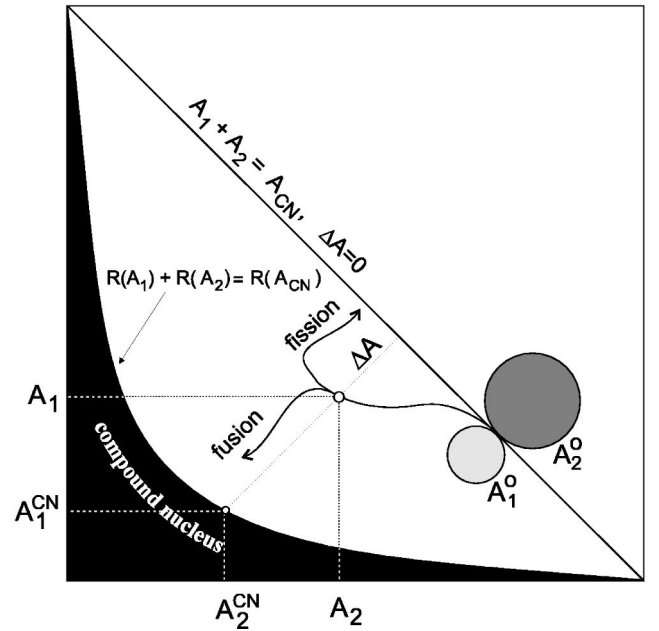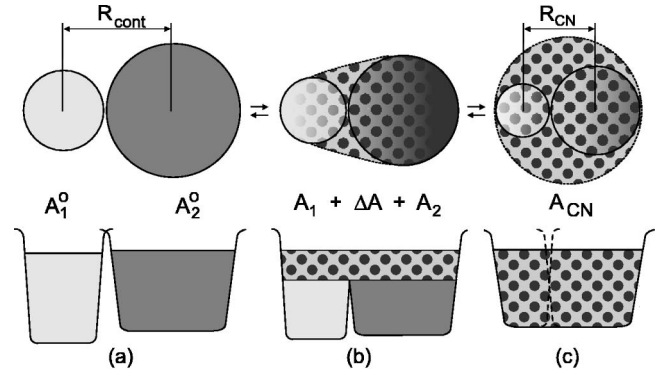

FIG. 7. Schematic view of the process of compound nucleus formation and fission in the space of A_1, A_2, and ΔA, i.e., the number of nucleons in the projectilelike nucleus, targetlike nucleus, and collectivized nucleons, here $A_1 + A_2 + \Delta A = A_{CN}$. Other notations are in the text.

ons with lower energies remain in the volumes of original nuclei. Subsequent evolution of the system cannot be described within such a simple model and needs including additional degrees of freedom, and, first of all, a greater number of interacting nucleons and nuclear surface deformations. All this makes even a classical problem difficult to solve.

Thus, basing on the model calculations, we may conclude that the concept of a "di-nuclear system" in which two touching nuclei keep their individualities during compound nucleus formation [11–13] seems to be too simplified.

VI. COLLECTIVIZATION AND DECOLLECTIVIZATION OF NUCLEONS AS A MECHANISM OF FUSION AND FISSION OF HEAVY NUCLEI

The following mechanism can be proposed as an alternative concept of the compound nucleus formation in competition with the quasifission process, see schematic Fig. 7.

(1) Down to the instant of touch the nuclei keep their individualities and the potential energy of their interaction is

defined in a usual manner as described above in Sec. II. The point of contact R_{cont} can be defined as the sum of nuclear radii that is smaller by $1-3$ fm than the radius of the Coulomb barrier and, thus, the nuclei have to overcome this barrier to reach it.

(2) In the point of contact the nuclei begin to lose their individualities due to an increasing number of common nucleons ΔA, here $A_1 + A_2 + \Delta A = A_{CN}$ [configuration (b) in Fig. 7]. Interaction of two touching nuclei A_1 and A_2 weakens with increasing the number of common nucleons ΔA, and their specific binding energies approach a specific binding energy of the compound nucleus. Collectivized nucleons move in the whole volume occupied by the two nuclei and have the average over A_1 and A_2 specific binding energy.

(3) Thus, the process of compound nucleus formation in competition with quasifission occurs in the space (A_1, A_2), here the compound nucleus is finally formed when two fragments A_1 and A_2 go in its volume, i.e., at $R(A_1) + R(A_2) = R(A_{CN}) \equiv R_{CN}$ or at $A_1^{1/3} + A_2^{1/3} = A_{CN}^{1/3}$ [configuration (c) in Fig. 7]. Let us denote these values as A_1^{CN} and A_2^{CN}, see Fig. 7.

For calculating the total energy of the nuclear system consisting of two nuclei surrounded by a certain number of common nucleons, the following expression can be used based on the concept formulated above and providing a continuity of the total energy at all the reaction stages beginning from the asymptotic state of two separate nuclei and up to the moment of the compound nucleus formation:

$$V_{fus-fis}[r = R(A_1) + R(A_2); A_1, A_2; \beta_1, \beta_2]$$
$$= V_{12}^{CN}(r; A_1, A_2, \beta_1, \beta_2) + B(A_1^0) + B(A_2^0)$$
$$- [\tilde{b}_1(\Delta A)A_1 + \tilde{b}_2(\Delta A)A_2 + \tilde{b}_{CN}(\Delta A)\Delta A].$$
$$(7)$$

Here $B(A_1^0)$ and $B(A_2^0)$ are the binding energies of the projectile and target; $\tilde{b}_1$, $\tilde{b}_2$, and $\tilde{b}_{CN} = (\tilde{b}_1 + \tilde{b}_2)/2$ are the specific binding energies of the nucleons in the fragments A_1, A_2, and that of the common nucleons ΔA, respectively. These quantities depend on the number of collectivized nucleons. At the border line $\Delta A = 0$, i.e., at $A_1 + A_2 = A_{CN}$, $\tilde{b}_{1,2} = B(A_{1,2}^0)/A_{1,2}^0 \equiv b_{1,2}^0$. At the moment of the compound nucleus formation, i.e., at $A_1^{1/3} + A_2^{1/3} \leqslant A_{CN}^{1/3}$ (the dark area in Fig. 7) the specific binding energy of all the nucleons is the same and equal to the specific binding energy of the compound nucleus: $\tilde{b}_1 = \tilde{b}_2 = \tilde{b}_{CN} = B(A_{CN})/A_{CN} \equiv b_{CN}$. Introducing the notations $\Delta A_{CN} = A_{CN} - A_1^{CN} - A_2^{CN}$ (see Fig. 7) and $x = (\Delta A_{CN} - \Delta A)/\Delta A_{CN}$, which is the parameter characterizing the remoteness of the system from the compound nucleus configuration, one can use a continuous approximation of $\tilde{b}_1$ and $\tilde{b}_2$ in the intermediate region $0 \leqslant x \leqslant 1$ in the following form:

$$\tilde{b}_{1,2} = b_{CN} + (b_{1,2} - b_{CN})\varphi(x), \qquad (8)$$

where $\varphi(x)$ is an appropriate monotonous function satisfying the conditions $\varphi(x=0)=0$ and $\varphi(x=1)=1$. A microscopic

description of the nuclear configuration (b) in Fig. 7 should be used to determine an explicit shape of this function. The simplest linear dependence $\varphi(x) = x$ was used here, and we found that some variation of it does not change significantly a common behavior and the main features of the function $V_{fus-fis}(A_1, A_2)$.

Potential energy of the interaction of two nuclei surrounded with a certain number of common nucleons, the first term in Eq. (7), is known along with its first derivative at the point of contact, i.e., at the borderline $\Delta A = 0$. When a uniform compound nucleus is formed, inside which the nuclei A_1 and A_2 are only conditionally isolated, their interaction is naturally equal to zero. In the intermediate region this interaction can be also approximated by a smooth function. Here a four-order polynomial was used providing a continuity of the interaction potential along with its first derivative (continuity of the force)

$$V_{12}^{CN}(r; A_1, A_2; \beta_1, \beta_2) = \begin{cases} V_{12}(r; \beta_1, \beta_2), & r \geqslant R_{cont} \\ c_1 \xi^2 + c_2 \xi^4, & \xi = r - R_{CN} \\ 0, & r \leqslant R_{CN}. \end{cases}$$
$$(9)$$

The interaction $V_{12}(r; \beta_1, \beta_2)$ has been discussed above in Sec. II. The parameters c_1 and c_2 are derived unambiguously from continuity of V_{12}^{CN} and its derivative in the point of the contact $r = R_{cont}$. Thus, once the compound nucleus has been formed (the dark area in Fig. 7), the total energy of the system is equal to $V_{fus-fis} = Q_{gg}^{fus} \equiv B(A_1^0) + B(A_2^0) - B(A_{CN})$, as it should be if the energy of two resting at infinity initial nuclei A_1^0 and A_1^0 is taken as zero.

The total driving potential $V_{fus-fis}$, which regulates the fusion-fission dynamics, depends on six variables $Z_1, N_1, Z_2, N_2, \beta_1, \beta_2$, and only its one- or two-dimensional projections can be drawn for its visualization. In Fig. 8 the "radial" dependence of $V_{fus-fis}$ is shown for the systems ^{48}Ca$+^{248}$Cm and ^{110}Pd$+^{110}$Pd. The distance between two nuclei is a "good" variable only at $r > R_{cont}$, where the potential energy can be defined in the usual way; the proximity potential is used here (see Sec. II). After the moment at which the two nuclei touch each other, the nuclear system evolves in the space of (A_1, A_2) as described above. However, in the same way as one makes within a two-center shell model, we can define here the distance between the centers of two fragments as $r = R(A_1) + R(A_2)$ to demonstrate a continuity of the potential energy in the whole region. Fixing $Z_1 = Z_1^0, N_1 = N_1^0$, and changing only Z_2 (with an optimal choice of N_2 to minimize the total energy) we calculated the potential $V_{fus-fis}$ at zero deformations and at $\beta = \beta_{sd}/2$. Here β_{sd} means the entrance channel saddle point deformation (see Fig. 1). The resulting potentials are shown in Fig. 8.

Fast decrease of the potential energy in the asymmetric system ^{48}Ca$+^{248}$Cm in the direction of the compound nucleus formation does not lead automatically to a large value of the corresponding probability P_{CN}, because after reaching the deep minimum at $r \sim 10$ fm the nuclear system evolves predominantly into the quasifission channels (see below Fig. 9). For the symmetric system ^{110}Pd$+^{110}$Pd [Fig.

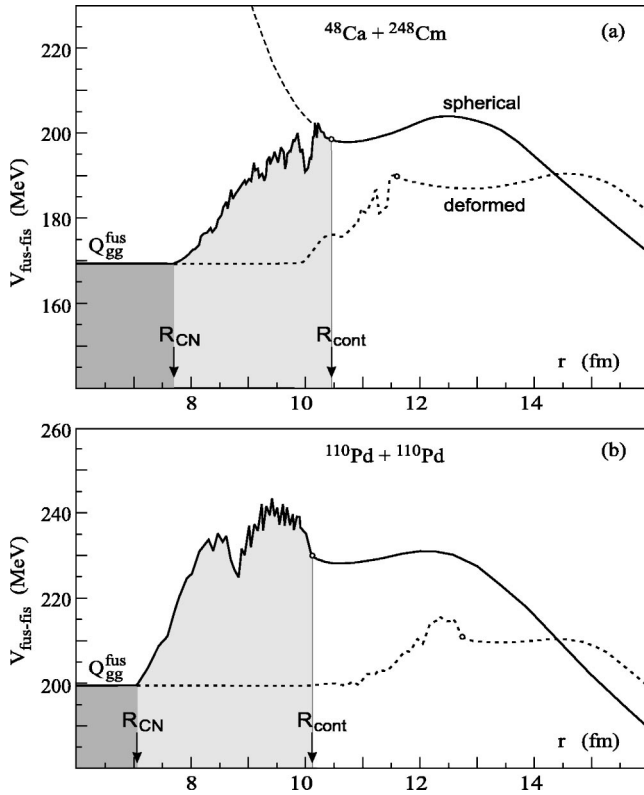FIG. 8. "Radial" dependence of the nucleus-nucleus potential energy $V_{fus-fis}$ for ^{48}Ca$+^{248}$Cm (a) and ^{110}Pd$+^{110}$Pd (b) calculated at zero deformations of the fragments (solid curves) and at $\beta=\beta_{sd}/2$ (dotted curves). At $r>R_{cont}$ the interaction of two separate nuclei is defined by a standard proximity potential V_{12} (at $r<R_{cont}$ this potential is shown by the dashed line). In the region $R_{CN}<r<R_{cont}$ (light-gray-shaded area) the distance between two touching nuclei is determined as $r=R(A_1)+R(A_2)$, here one nucleus is fixed ($A_1=A_1^0$, $Z_1=Z_1^0$) while the other is varied, i.e., the potential energy at $r<R_{cont}$ in the case (a) is calculated along the horizontal line $Z_1=20$ in Fig. 9. The deep minimum at $r\sim10$ fm corresponds to the configuration marked by the cross in Fig. 9.

8(b)] the total potential energy $V_{fus-fis}$ reveals an additional barrier at $r<R_{cont}$, which reflects unfavorableness for these two nuclei to collectivize the nucleons due to decrease of the total binding energy. The other characteristic feature of the potential energy in that case is the very low "locked" barrier (or shallow pocket), which cannot prevent the two touching nuclei to break apart. Both these facts lead to decrease of the fusion probability for these nuclei at low colliding energy. Dynamic deformation of the nuclei aggravates even more the situation for symmetrical system [see dotted curve in Fig. 8(b)]. For heavier nearly symmetrical nuclei (e.g., ^{136}Xe $+^{136}$Xe) in the case of dynamic prolate deformations the potential energy in the point of contact becomes lower than the energy of the ground state of the compound nucleus Q_{gg}, which makes their fusion quite improbable at low near-barrier collision energies.

The topographical landscape of the total energy $V_{fus-fis}$ for the case of formation of the compound nucleus ^{296}116 is shown in Fig. 9. One can see that the shell structure, clearly
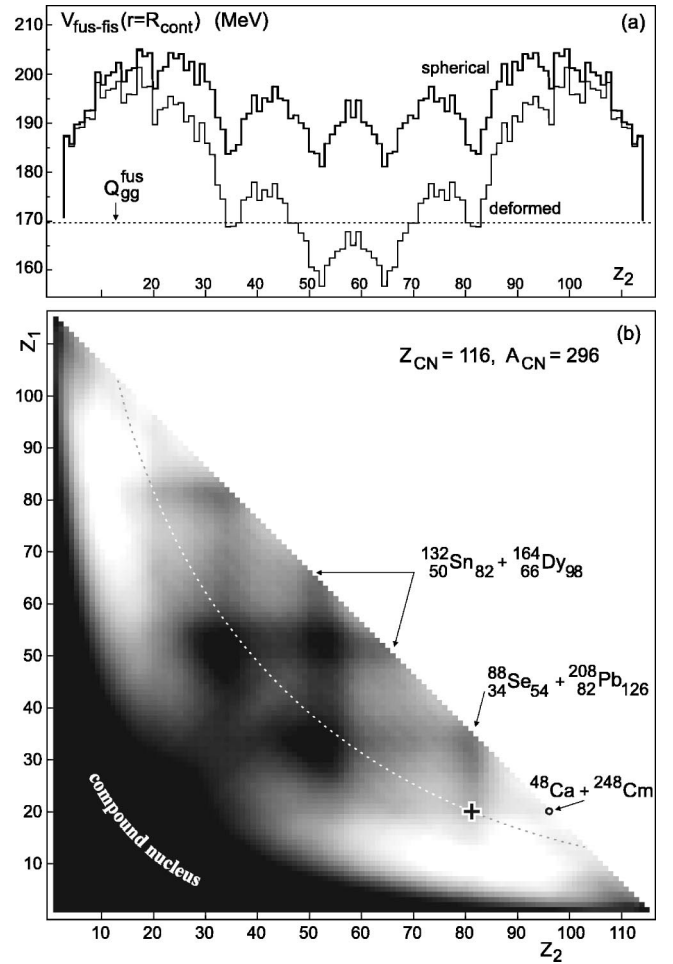

FIG. 9. The driving potential $V_{fus-fis}(Z_1,Z_2)$ of the nuclear system consisting of 116 protons and 180 neutrons (see the text). (a) Potential energy of two touching nuclei at $A_1+A_2=A_{CN},\Delta A=0$, i.e., along the diagonal of the lower figure. The thick line corresponds to the case of spherical nuclei, whereas the thin line corresponds to $\beta=\beta_{sd}/2$. (b) Topographical landscape of the driving potential on the plane (Z_1,Z_2) (zero deformation). The dark regions correspond to the lower potential energies. The dotted line passes through the configurations with $R(A_1)+R(A_2)=10$ fm (see Fig. 10).

revealing itself in the contact of two nuclei, i.e., at the borderline $A_1+A_2=A_{CN}$ [Fig. 9(a)], is also retained at $\Delta A\neq0$ [see, e.g., the deep minima in the regions of $Z_{1,2}=50$ and $Z_{1,2}=82$ in Fig. 9(b)]. From the figure it is already clear that in the synthesis of the nucleus ^{296}116 in the reaction ^{48}Ca $+^{248}$Cm, on the way from the contact point to the compound nucleus formation (dark area) the system has to decay with a large probability into the quasifission channels (Se+Pb, Kr +Hg) or into the channels of normal fission (Sn+Dy, Te +Gd)—shadowed regions in Fig. 9(b). As the calculations show, the most part of incoming flux goes from the point of contact [marked by the small circle in Fig. 9(b)] along the ravine $Z_1=20$ (decreasing mass and charge of the heavy fragment) up to the point marked by the cross ($Z_2\sim82$). After that the flux turns into the deeper valley of the potential energy, going along $Z_2\sim82$ with increasing the mass and
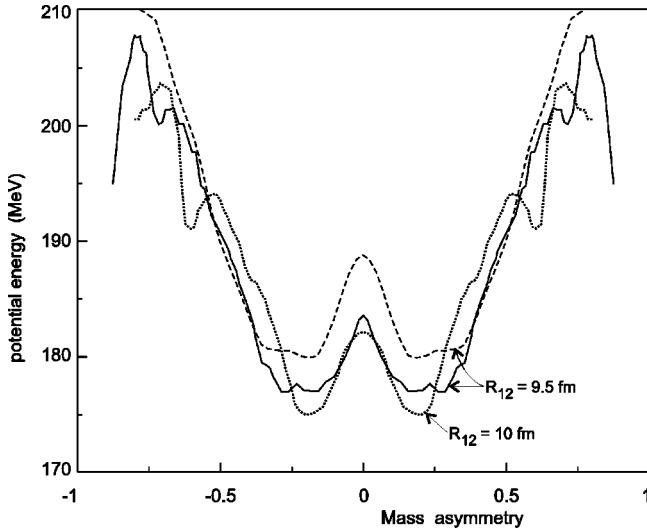
FIG. 10. Dependence of the driving potential $V_{fus-fis}$ on mass asymmetry. Driving potential (7) was calculated at zero deformation for $R(A_1)+R(A_2)=9.5$ fm (solid line) and 10 fm (dotted line). The last case corresponds to the nuclear configurations shown by the dotted line in Fig. 9. The dashed line shows the driving potential calculated within the two-center shell model approach [37,38] at $R_{12}=9.5$ fm.
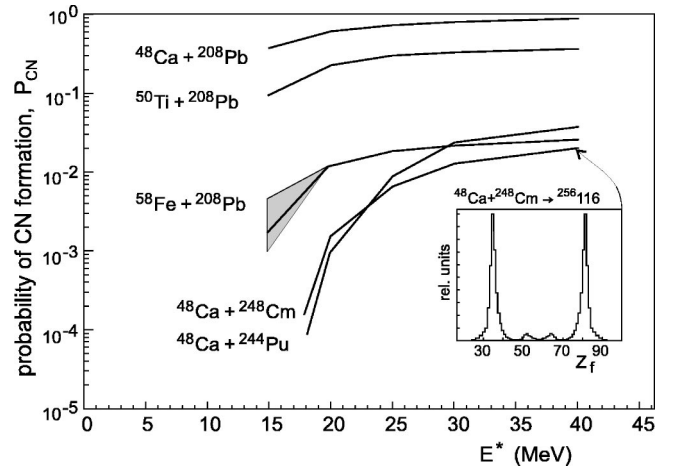

FIG. 11. The probability of the compound nucleus formation for the near-barrier fusion reactions. In the inset the corresponding charge distribution of quasifission fragments is shown for the ^{48}Ca+^{248}Cm fusion reaction at $E^*=40$ MeV (linear scale, relative units).

charge of the light fragment, and comes to the quasifission exit channels with the heavier fragment in the region of ^{208}Pb (see below the quasifission charge distribution in Fig. 11). Only a small part of the incoming flux reaches a compound nucleus configuration.

In [37] a shape of dinuclear system was described by the three collective parameters [deformation of the fragments, distance between centers, and mass asymmetry $\alpha=(A_1-A_2)/(A_1+A_2)$], and the potential energy was calculated then within a two-center shell model approach [38] as a sum of the LD potential energy plus the shell correction. Due to close physical meaning of the used parameters the driving potential (7) can be compared with that calculated in [37]. Result of such comparison is shown in Fig. 10 by the solid and dashed curves. As can be seen, the two potentials are close both in absolute values and in their behavior. A difference is found for large mass asymmetry and for the configurations close to the point of contact (or scission point), where a two-center shell model produces not-so-good result due to using unrealistic nuclear shapes [37]. For that cases the driving potential (7) seems to be more appropriate, whereas for the configurations with a large number of collectivized nucleons (region of the fission saddle point) a two-center shell model calculations should be more reliable. The driving potential (7) has a more pronounced structure, reflecting the shell effects (for example, deep minimum at $R_{12}=10$ fm and $\alpha\approx0.6$ corresponds to the ^{208}Pb valley in Fig. 9), and also the strongly marked Businaro-Gallone point.

Knowing the driving potential $V_{fus-fis}(Z_1,N_1,Z_2,N_2;\beta_1,\beta_2)$ and the excitation energy of the system in every point we can now determine the probability of the compound nucleus formation $P_{CN}(A_1^0+A_2^0\rightarrow C)$, being part of expression (1) for the cross section of the synthesis of superheavy

nuclei. It can be done, for example, by solving the corresponding Fokker-Planck equation or master equation for the distribution function $F(\vec{y}=\{Z_1,N_1,Z_2,N_2,\beta_1,\beta_2\};t)$. The probability of the compound nucleus formation is determined as an integral of the distribution function $F(\vec{y}=\{Z_1,N_1,Z_2,N_2\};t)$ over the region $R(A_1)+R(A_2)\leq R_{CN}$. Similarly one can define the probabilities of finding the system in different channels of quasifission or normal fission, i.e., the charge and mass distribution of fission fragments measured in experiments. In fact, it is not so easy to perform such realistic calculations due to the large number of the variables. The initial and the boundary conditions should also be defined very accurately to split incoming flux into the three very unequal parts: quasielastic scattering, fusion, and quasifission. In the case of solving the Fokker-Planck equation, we should also smooth somehow a shaggy dependence of the driving potential on proton and neutron numbers to calculate the corresponding partial derivatives.

Here the master equation approach with restricted number of the variables was used for a rough estimation of P_{CN} and evolution of the nuclear system in the (Z_1,Z_2) space. Putting $\beta=\beta_{sd}/2$ and minimizing the potential energy over N_1 and N_2, we calculated the two-dimensional driving potential $V_{fus-fis}(Z_1,Z_2)$, which defines the master equation for the distribution function $F(y=\{Z_1,Z_2\},t)$ [39]

$$\frac{\partial F}{\partial t}=\sum_{y'}\lambda(y,y')F(y',t)-\lambda(y',y)F(y,t). \quad (10)$$

We use the same macroscopic transition probabilities as in [39], i.e., $\lambda(y,y')\sim\exp\{[V_{fus-fis}(y')-V_{fus-fis}(y)]/2T\}$, where $T=\sqrt{[E_{c.m.}-V_{fus-fis}(y)]/a}$ is the temperature and a is the level density parameter. The sum over y' in Eq. (10) is extended only to nearest configurations $Z_{1,2}\pm1$. At $t=0$, $F(Z_1=Z_1^0,Z_2=Z_2^0)=1$, and $F(Z_1,Z_2)=0$ for all other values of Z_1 and Z_2. Equation (10) was solved up to the mo-

ment when the total flux comes to the compound nucleus configurations [dark area in Fig. 9(b)] and/or escapes into the fission channels giving the probability for the compound nucleus formation and the charge distribution of quasifission fragments. Decay of the system into the quasielastic channels with $Z_1 \sim Z_1^0$ and $Z_2 \sim Z_2^0$ was suppressed by appropriate boundary condition to provide a correct normalization for P_{CN}.

Calculation results are shown in Fig. 11 for the reactions $^{48}\text{Ca}+^{208}\text{Pb}\rightarrow^{256}\text{No}$, $^{50}\text{Ti}+^{208}\text{Pb}\rightarrow^{258}\text{Rf}$, $^{58}\text{Fe}+^{208}\text{Pb}\rightarrow^{266}\text{Hs}$, $^{48}\text{Ca}+^{244}\text{Pu}\rightarrow^{292}114$, and $^{48}\text{Ca}+^{248}\text{Cm}\rightarrow^{296}116$ depending on the excitation energy. Note that for the low excitation energies ($E^*<20$ MeV) an accuracy of the solution of the master equation (10) is not so high. A typical uncertainty is shown by the shadowed area in Fig. 11 for the case of $^{58}\text{Fe}+^{208}\text{Pb}$. The following conclusions could be made from these results. At $Z_{CN}>102$ the probability of the compound nucleus formation decreases very fast with increasing the charge of the projectile at the fixed ^{208}Pb target nucleus. In more asymmetric fusion reactions with a ^{48}Ca projectile a decrease in P_{CN} is not so drastic with increasing Z_{CN} at near-barrier collision energies. It means that P_{CN} does not depend much on the charge of the compound nucleus, but mainly on the combination of fusing nuclei. For asymmetric systems considered here, the probability of the compound nucleus formation increases very fast with increasing the excitation energy, but it is almost saturated at $E^*>25$ MeV. The charge distribution of quasifission fragments (see the inset in Fig. 11) mainly reflects the corresponding potential energy at the contact point, and the probability for the symmetric quasifission is not negligible. It means that for some reactions it is rather difficult to distinguish experimentally between the normal fission (which is a measure for the fusion cross section) and the quasifission process.

Putting the obtained values of P_{CN} into Eq. (1) we calculated the cross sections of heavy ER formation in the reactions $^{48}\text{Ca}+^{208}\text{Pb}\rightarrow^{256}\text{No}$, $^{50}\text{Ti}+^{208}\text{Pb}\rightarrow^{258}\text{Rf}$, $^{58}\text{Fe}+^{208}\text{Pb}\rightarrow^{266}\text{Hs}$, and $^{48}\text{Ca}+^{244}\text{Pu}\rightarrow^{292}114$ and obtained satisfactory agreement with experimental data (see the dashed curves in Figs. 2–4, 12). In the synthesis of element 114 it was found that ER cross sections at $E^*\leqslant30$ MeV do not exceed 1 pb [1]. As can be seen from Fig. 12, the calculated ER cross sections overestimate this value. It could be explained by overestimating the fission barrier used for the calculation of the survival probability of the $^{292}114$ nucleus. The shell correction $\delta W=8.9$ MeV predicted in [30] for that nucleus is very high. In [31] the value of the same quantity was found to be by 2 MeV lower. The dotted curves in Fig. 12 show the result of a reduction of the fission barrier by 1 MeV, which is justified here due to a large uncertainty of this quantity. Thus we may finally conclude that the probabilities of the compound nucleus formation calculated within the proposed approach agree rather well with experimental data on the synthesis of superheavy nuclei in the asymmetric fusion reactions.

VII. CONCLUSION

The synthesis of superheavy easily fissile nuclei is a difficult many-sided physics problem, in which not only some
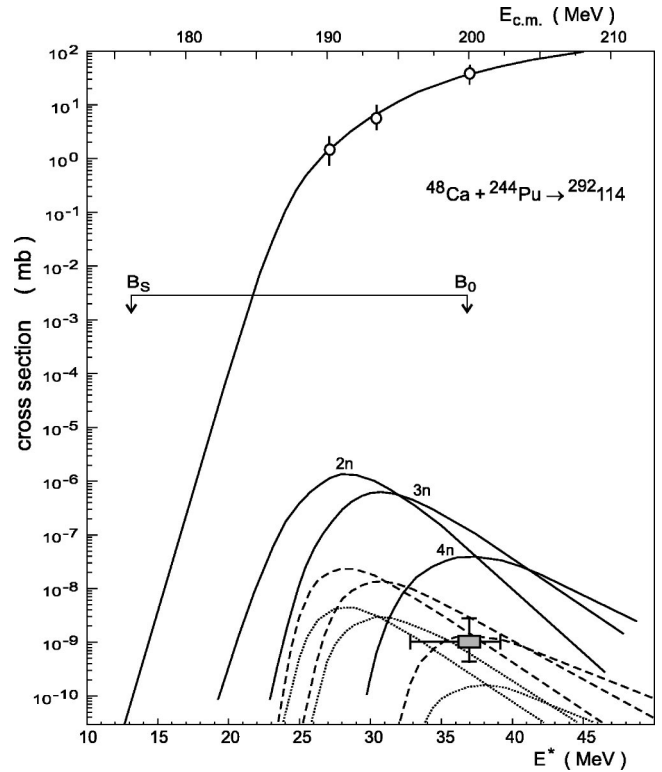

FIG. 12. (a) The capture cross section and formation cross sections for evaporation residues in the $^{48}\text{Ca}+^{244}\text{Pu}$ reaction. Experimental data on the capture cross sections are from [35]. The experimental point for the $^{288}114$ nucleus formation in the $4n$ evaporation channel is from [1]. The solid curves show the results obtained with $P_{CN}=1$ whereas the dashed curves correspond to the P_{CN} values shown in Fig. 11. Result of subsequent reduction of the fission barrier by 1 MeV (see the text) are shown by the dotted curves.

quantities crucially influencing the whole process are poorly determined but also the dynamics of the process itself. For better understanding of the role of dynamic deformations and nucleon transfer in the course of overcoming the multidimensional potential barrier, additional experimental and theoretical investigations are undoubtedly required. Decay properties of the superheavy nuclei and, first of all, the heights of their fission barriers are also poorly studied and, as a matter of fact, are almost free theoretical parameters in specific calculations.

However, analysis of available experimental data performed employing a rather accurate theoretical approach with the use of realistic parameters and without any additional fitting of these latter shows that the fusion process of asymmetric nuclei resulting in the formation of very heavy elements up to $Z=102$ differs only insignificantly from the fusion of light and medium nuclei, when a compound nucleus is formed with a probability close to unity once the nuclei have overcome the multidimensional potential barrier. In the asymmetric synthesis of superheavy elements with $Z_{CN}\geqslant104$ and also in the fusion of heavy symmetric nuclei with $Z_{CN}\geqslant90$ the process of the compound nucleus formation itself plays an important role due to a strong competition with the processes of fission and quasifission.

A new mechanism of the fusion-fission process for heavy

nuclear systems has been proposed. It takes place in the space (A_1, A_2), where A_1 and A_2 are two nuclei surrounded by a certain number of common nucleons ΔA. These two nuclei gradually lose (or acquire) their individualities with increasing (or decreasing) the number of collectivized nucleons ΔA, here ''individuality'' means mainly a specific binding energy of the nucleons inside the nuclei A_1 and A_2, which decreases when a heavy compound nucleus is being formed and increases when it undergoes fission. The corresponding driving potential has been derived. It regulates the behavior of the system in the (A_1, A_2) space and allows the calculation of both the probability of the compound nucleus formation and the mass distribution of fission fragments in the heavy ion fusion reactions. For the compact nuclear configurations this potential is very similar to the driving potential calculated within a two-center shell model approach and differs from it at large values of mass asymmetry and also for the configurations close to the point of contact of two nuclei. Numerical calculations of the fusion probability allowed to reproduce experimental data on the yield of superheavy nuclei in heavy ion fusion reactions.

[1] Yu. Ts. Oganessian, V. K. Utyonkov, Yu. V. Lobanov, F. Sh. Abdulin, A. N. Polyakov, I. V. Shirokovsky, Yu. S. Tsyganov, G. G. Gulbekian, S. L. Bogomolov, B. N. Gikal, A. N. Mezentsev, S. Iliev, V. G. Subbotin, A. M. Sukhov, G. V. Buklanov, K. Subotic, M. G. Itkis, K. J. Moody, J. F. Wild, N. J. Stoyer, M. A. Stoyer, and R. W. Lougheed, Phys. Rev. Lett. **83**, 3154 (1999).

[2] Yu. Ts. Oganessian, A. V. Yeremin, A. G. Popeko, S. L. Bogomolov, G. V. Buklanov, M. L. Chelnokov, V. I. Chepigin, B. N. Gikal, V. A. Gorshkov, G. G. Gulbekian, M. G. Itkis, A. P. Kabachenko, A. Yu. Lavrentev, O. N. Malyshev, J. Rohac, R. N. Sagaidak, S. Hofmann, S. Saro, G. Giardina, and K. Morita, Nature (London) **400**, 242 (1999).

[3] V. Ninov, K. E. Gregorich, W. Loveland, A. Ghiorso, D. S. Hoffman, D. M. Lee, H. Nitsche, W. J. Swiatecki, U. W. Kirbach, C. A. Laue, J. L. Adams, J. B. Patin, D. A. Shaughnessy, D. A. Strellis, and P. A. Wilk, Phys. Rev. Lett. **83**, 1104 (1999).

[4] S. Hofmann and G. Munzenberg, Rev. Mod. Phys. **72**, 733 (2000).

[5] J. Tōke, R. Bock, G. X. Dai, S. Gralla, A. Gobbi, K. D. Hildenbrand, J. Kuzminski, W. F. J. Müller, H. Stelzer, B. B. Bock, and S. Bjørnholm, Nucl. Phys. **A440**, 327 (1985).

[6] W. J. Swiatecki, Phys. Scr. **24**, 113 (1981).

[7] S. Bjornholm and W. J. Swiatecki, Nucl. Phys. **A391**, 471 (1982).

[8] J. Blocki, H. Feldmeier, and W. J. Swiatecki, Nucl. Phys. **A459**, 145 (1986).

[9] Y. Aritomo, T. Wada, M. Ohta, and Y. Abe, Phys. Rev. C **59**, 796 (1999).

[10] V. Yu. Denisov and S. Hofmann, Phys. Rev. C **61**, 034606 (2000).

[11] N. V. Antonenko, E. A. Cherepanov, A. K. Nasirov, V. P. Permjakov, and V. V. Volkov, Phys. Lett. B **319**, 425 (1993); Phys. Rev. C **51**, 2635 (1995).

[12] G. G. Adamjan, N. V. Antonenko, W. Scheid, and V. V. Volkov, Nucl. Phys. **A627**, 361 (1997).

[13] E.A. Cherepanov, JINR Report No. E7-99-27, 1999.

[14] M. Dasgupta, D. J. Hinde, N. Rowley, and A. M. Stefanini, Annu. Rev. Nucl. Part. Sci. **48**, 401 (1998).

[15] R. Bass, *Nuclear Reactions with Heavy Ions* (Springer-Verlag, Berlin, 1980), p. 326.

[16] V. I. Zagrebaev, N. S. Nikolaeva, and V. V. Samarin, Izv. Akad. Nauk, Ser. Fiz. **61**, 2157 (1997).

[17] J. Blocki, J. Randrup, W. J. Swiatecki, and C. F. Tsang, Ann. Phys. (N.Y.) **105**, 427 (1977).

[18] D. L. Hill and J. A. Wheeler, Phys. Rev. **89**, 1102 (1953).

[19] N. Rowley, G. R. Satchler, and P. H. Stelson, Phys. Lett. B **254**, 25 (1991).

[20] A.V. Ignatyk, *Statistical Properties of Excited Atomic Nuclei* (Energoatomizdat, Moscow, 1983).

[21] K.-H. Schmidt and W. Morawek, Rep. Prog. Phys. **54**, 949 (1991).

[22] A. R. Junghans, M. de Jong, H.-G. Clerc, A. V. Ignatyuk, G. A. Kudyaev, and K.-H. Schmidt, Nucl. Phys. **A629**, 635 (1998).

[23] E. A. Cherepanov and A. S. Iljinov, Nukleonika **A25**, 611 (1980).

[24] M. Blann, Nucl. Phys. **80**, 223 (1966).

[25] J. R. Grover and J. Gilat, Phys. Rev. **157**, 802 (1967).

[26] J. Gomez del Campo, Phys. Rev. Lett. **36**, 1529 (1976).

[27] G. Audi and A. H. Wapstra, Nucl. Phys. **A595**, 409 (1995).

[28] W. D. Myers and W. J. Swiatecki, Ark. Fys. **36**, 343 (1967).

[29] W. D. Myers and W. J. Swiatecki, Table of Nuclear Masses According to the 1994 Thomas-Fermi Model, Report No. LBL-36803, 1994.

[30] P. Möller, J. R. Nix, W. D. Myers, and W. J. Swiatecki, At. Data Nucl. Data Tables **59**, 185 (1995).

[31] R. Smolanczuk, J. Skalski, and A. Sobiczewski, GSI Report No. GSI-94-77, 1994; R. Smolanczuk, Phys. Rev. C **56**, 812 (1997).

[32] M. G. Itkis, Yu. Ts. Oganessian, E. M. Kozulin, N. A. Kondratiev, L. Krupa, I. V. Pokrovsky, A. N. Polyakov, V. A. Ponomarenko, E. V. Prokhorova, B. I. Pustylnik, A. Ya. Rusanov, and I. V. Vakatov, Nuovo Cimento A **111**, 783 (1998).

[33] A. V. Yeremin, V. I. Chepigin, M. G. Itkis, A. P. Kabachenko, S. P. Korotkov, O. N. Malyshev, Yu. Ts. Oganessian, A. G. Popeko, J. Rohac, R. N. Sagaidak, M. L. Chelnokov, V. A. Gorshkov, A. Yu. Lavrentev, S. Hofmann, G. Munzenberg, M. Veselsky, S. Saro, K. Morita, N. Iwasa, S. I. Mulgin, and S. V.

Zhdanov, JINR Report No. 6[92]-98, 1998.

[34] S. Hofmann, Rep. Prog. Phys. **61**, 639 (1998).

[35] M. G. Itkis, Yu. Ts. Oganessian, A. A. Bogatchev, I. M. Itkis, M. Jandel, J. Kliman, G. N. Kniajeva, N. A. Kondratiev, I. V. Korzyukov, E. M. Kozulin, L. Krupa, I. V. Pokrovski, E. V. Prokhorova, B. I. Pustylnik, A. Ya. Rusanov, V. M. Voskresenski, F. Hanappe, B. Benoit, T. Materna, N. Rowley, L. Stuttge, G. Giardina, and K. J. Moody, in *Proceedings on Fusion Dynamics at the Extremes, Dubna, 2000*, edited by Yu. Oganessian and V. Zagrebaev (World Scientific, Singapore, 2001), p. 93.

[36] C.-C. Sahm, H.-G. Clerc, K.-H. Schmidt, W. Reisdorf, P. Armbruster, F. P. Heßberger, J. G. Keller, G. Münzenberg, and D. Vermeulen, Nucl. Phys. **A441**, 316 (1985).

[37] Y. Aritomo, T. Wada, M. Ohta, and Y. Abe, in *Proceedings on Fusion Dynamics at the Extremes, Dubna, 2000* (Ref. [35]), p. 123.

[38] S. Suekane, A. Iwamoto, S. Yamaji, and K. Harada, JAERI-memo 5918, 1974; A. Iwamoto, S. Yamaji, S. Suekane, and K. Harada, Prog. Theor. Phys. **55**, 115 (1976).

[39] L. G. Moretto and J. S. Sventek, Phys. Lett. **58B**, 26 (1975).